



HAL
open science

Two Distinct Gb3/CD77 Signaling Pathways Leading to Apoptosis Are Triggered by Anti-Gb3/CD77 mAb and Verotoxin-1

Cécile Tétaud, Thomas Falguières, Karine Carlier, Yann Lécluse, Julie Garibal, Dominique Coulaud, Pierre Busson, Rudi Steffensen, Henrik Clausen, Ludger Johannes, et al.

► To cite this version:

Cécile Tétaud, Thomas Falguières, Karine Carlier, Yann Lécluse, Julie Garibal, et al.. Two Distinct Gb3/CD77 Signaling Pathways Leading to Apoptosis Are Triggered by Anti-Gb3/CD77 mAb and Verotoxin-1. *Journal of Biological Chemistry*, 2003, 278 (46), pp.45200 - 45208. <10.1074/jbc.m303868200>. <inserm-05570684>

HAL Id: inserm-05570684

<https://inserm.hal.science/inserm-05570684v1>

Submitted on 27 Mar 2026

HAL is a multi-disciplinary open access archive for the deposit and dissemination of scientific research documents, whether they are published or not. The documents may come from teaching and research institutions in France or abroad, or from public or private research centers.

L'archive ouverte pluridisciplinaire HAL, est destinée au dépôt et à la diffusion de documents scientifiques de niveau recherche, publiés ou non, émanant des établissements d'enseignement et de recherche français ou étrangers, des laboratoires publics ou privés.



Distributed under a Creative Commons CC BY 4.0 - Attribution - International License

Two Distinct Gb3/CD77 Signaling Pathways Leading to Apoptosis Are Triggered by Anti-Gb3/CD77 mAb and Verotoxin-1*

Received for publication, April 14, 2003, and in revised form, August 26, 2003
Published, JBC Papers in Press, August 27, 2003, DOI 10.1074/jbc.M303868200

Cécile Tétaud‡, Thomas Falguières§, Karine Carlier‡¶, Yann Lécluse||, Julie Garibal‡, Dominique Coulaud‡, Pierre Busson‡, Rudi Steffensen**, Henrik Clausen**, Ludger Johannes§, and Joëlle Wiels‡ ††

From the ‡Laboratoire Interactions Moléculaires et Cancer, CNRS UMR 8126, Institut Gustave Roussy, 94805 Villejuif cedex, France, the §Unité Mixte de Recherche 144, Institut Curie, 26 rue d'Ulm, 75248 Paris cedex 05, France, the ||Service Commun de Cytométrie, Institut Fédératif de Recherche 54, Institut Gustave Roussy, 94805 Villejuif cedex, France, and the **School of Dentistry, University of Copenhagen, Norre Allé 20, 2200 Copenhagen N, Denmark

Globotriaosylceramide (Gb3), a neutral glycosphingolipid, is the B-cell differentiation antigen CD77 and acts as the receptor for most Shiga toxins, including verotoxin-1 (VT-1). We have shown that both anti-Gb3/CD77 mAb and VT-1 induce apoptosis in Burkitt's lymphoma cells. We compared the apoptotic pathways induced by these two molecules by selecting cell lines sensitive to only one of these inducers or to both. In all these cell lines (including the apoptosis-resistant line), VT-1 was transported to the endoplasmic reticulum and inhibited protein synthesis similarly, suggesting that VT-1-induced apoptosis is dissociated from these processes. VT-1 triggered a caspase- and mitochondria-dependent pathway (rapid activation of caspases 8 and 3 associated with a loss of mitochondrial membrane potential ($\Delta\psi_m$) and the release of cytochrome *c* from mitochondria). In contrast, the anti-Gb3/CD77 mAb-induced pathway was caspase-independent and only involved partial depolarization of mitochondria. Antioxidant compounds had only marginal effects on VT-1-induced apoptosis but strongly protected cells from anti-Gb3/CD77 mAb-induced apoptosis. VT-1- and anti-Gb3/CD77 mAb-treated cells displayed very different features on electron microscopy. These results clearly indicate that the binding of different ligands to Gb3/CD77 triggers completely different apoptotic pathways.

Globotriaosylceramide (Gb3: Gal α 1 \rightarrow 4Gal β 1 \rightarrow 4Glc β 1 \rightarrow Cer), a neutral glycosphingolipid (GSL),¹ has been identified as three different entities according to the cell type on which it is found. On erythrocytes, it constitutes the rare P^k blood group antigen (1). On lymphocytes, it constitutes the CD77 differentiation an-

tigen and its expression is limited to a subset of germinal center B cells (2, 3). On endothelial cells, it serves as the natural receptor for bacterial toxins of the Shiga family (Stx) (4). The function of Gb3/CD77 has been extensively investigated. We previously reported that the ligation of Gb3/CD77 by specific monoclonal antibodies (mAb) induces apoptosis in Burkitt's lymphoma (BL) cells, the tumoral counterparts of Gb3/CD77(+) germinal center B lymphocytes. We have also demonstrated that this apoptosis involves a rapid, sustained increase in intracellular Ca²⁺ concentration, a rapid, transient increase in cAMP levels, protein kinase A activation, and, finally, ceramide accumulation (5, 6).

Because Gb3/CD77 is the Shiga toxin receptor, numerous studies have analyzed the role of these toxins and their receptor in pathogenesis (reviewed in Ref. 7). In humans, infection by Stx-producing organisms (some strains of *Escherichia coli* and *Shigella dysenteriae* type 1) causes gastrointestinal diseases and the more serious hemolytic uremic syndrome, both of which are responsible for large numbers of deaths (reviewed in Refs. 4 and 8). Stx (also called verotoxins (VT) because the *E. coli* toxins were originally described to be cytotoxic to Vero cells (8)) are bipartite molecules comprised of an A catalytic subunit and five B subunits that specifically bind Gb3/CD77. The A subunit has RNA *N*-glycosidase activity; it removes an adenine base from 28 S RNA, thereby inhibiting protein synthesis and killing target cells (9). Several recent studies have demonstrated that these toxins also induce apoptosis in various cell types. These studies have led to an ongoing controversy about the relationship between apoptosis and cell death due to protein synthesis inhibition (10–13). Studies of Stx and Gb3/CD77 have also helped to elucidate intracellular transport events (14, 15). It has been shown that the targeting of the toxin to a specific intracellular transport pathway can be determined by the Gb3/CD77 isoform expressed on the cell surface and by the presence or absence of Gb3/CD77 in the lipid raft microdomains of the membrane (16, 17).

In this study, we investigated the nature of the apoptotic signals mediated by Gb3/CD77. Recent reports have shed light on both toxin- and anti-Gb3/CD77 mAb-induced apoptotic pathways (6, 18, 19), but various questions remain unresolved: Is ligand binding to Gb3/CD77 sufficient to induce apoptosis? Do ligands trigger a single intracellular mechanism? What is the relationship between protein synthesis inhibition and apoptosis for toxins? We investigated these issues by comparing the apoptotic mechanisms induced by anti-Gb3/CD77 mAb and verotoxin-1 (VT-1) in various BL cells. Cellular toxicity was strictly dependent on the expression of Gb3/CD77 on the cell surface in both cases, but some cell lines strongly expressing Gb3/CD77 were killed by both inducers, whereas others were

* This work was supported in part by grants from the Association pour la Recherche sur le Cancer (ARC 4213), the Ministère de la Recherche et des Nouvelles Technologies (ACI jeunes chercheurs-5223), and the Fondation de France. The costs of publication of this article were defrayed in part by the payment of page charges. This article must therefore be hereby marked "advertisement" in accordance with 18 U.S.C. Section 1734 solely to indicate this fact.

¶ Holds a doctoral fellowship from the Ligue Nationale Française contre le Cancer.

†† To whom correspondence should be addressed. Tel.: 33-1-42-11-47-40; Fax: 33-1-42-11-54-94; E-mail: wiels@igr.fr.

¹ The abbreviations used are: GSL, glycosphingolipid; BL, Burkitt's lymphoma; ER, endoplasmic reticulum; Gb3, globotriaosylceramide; GSH-EE, reduced glutathione ethyl ester; NAC, *N*-acetyl-L-cysteine; $\Delta\psi_m$, mitochondrial membrane potential; PPMP, 1-phenyl-2-palmitoylamino-3-morpholino-1-propanol; Stx, Shiga toxin family; VT-1, verotoxin-1; α 4Gal-T1, UDP-galactose: LacCer, α 1,4-galactosyltransferase; GD3, ganglioside GD3; LacCer, lactosyl ceramide.

only killed by one. Our results indicate that these two ligands trigger different signaling pathways: VT-1-induced apoptosis involves caspase activation and mitochondrial depolarization, whereas oxidative stress seems to mediate anti-G_b3/CD77 mAb-induced cell death. Finally, the ability of VT-1 to induce apoptosis was not correlated with the transport of this molecule to the endoplasmic reticulum (ER) or with the inhibition of protein synthesis.

EXPERIMENTAL PROCEDURES

Cell Lines—All cell lines used in this study were originally established from endemic or sporadic cases of Burkitt's lymphoma. The Ramos BL cell line was obtained from ATCC (Rockville, MD), whereas the Namalwa and P3HR1 cells lines were kindly provided by Prof. G. Klein (Stockholm, Sweden) and the BL2 cells by Prof. G. Lenoir (Lyon, France). These cell lines were cultured in RPMI 1640 medium (Invitrogen, France) containing 2 mM L-glutamine, 1 mM sodium pyruvate, 20 mM glucose, 100 units/ml penicillin, and 100 µg/ml streptomycin, and supplemented with 5% heat-inactivated fetal calf serum. G_b3/CD77(−) Ramos cells were obtained after 10 days of culture in media containing 2 µM PPMP (1-phenyl-2-palmitoylamino-3-morpholino-1-propanol HCl), a glucosylceramide synthase inhibitor causing reversible GSL depletion (20). PPMP was obtained from Matreya (Pleasant Gap, PA).

Reagents—1A4 ascites (mouse monoclonal IgM anti-G_b3/CD77) was provided by Dr. S. Hakomori (Seattle, WA) (21). IgM were purified with the Immunopure IgM purification kit (Pierce, Rockford, IL), according to the manufacturer's instructions. Purified recombinant verotoxin-1 (VT-1) was kindly provided by Dr. C. Lingwood (Toronto, Canada). The goat anti-human IgM (F(ab')₂ fragment) was purchased from Jackson ImmunoResearch Laboratories (West Grove, PA), the anti-cytochrome *c* mAb (clone 7H8.2C12) was from BD Pharmingen (Palo Alto, CA), the anti-PARP mAb (Ab-2, clone c-2-10) and the anti-caspase-8 mAb (Ab-3, clone 1-3) were from Oncogene Research Products (Boston, MA). The goat anti-mouse IgM (GAM), used to cross-linked 1A4 mAb in apoptosis experiments, was obtained from Pierce. The horseradish peroxidase-conjugated rabbit anti-mouse IgG (RAM), used for Western blotting, was from Zymed Laboratories Inc. (San Francisco, CA). The FITC-coupled goat anti-mouse IgG plus IgM, used for FACS analysis, was from Caltag Laboratory (Burlingame, CA). *N*-Acetyl-L-cysteine (NAC) and GSH ethyl ester (GSH-EE), a cell-permeable form of reduced glutathione (GSH), were purchased from Sigma (L'isle d'Abeau Chesnes, France). The fluorescent dye 3,3'-dihexyloxycarbocyanine iodide (DiOC₆ (3)) was obtained from Molecular Probes (Eugene, OR). A stock solution (1 mM in Me₂SO) was stored at room temperature. The peptide inhibitor of caspase 8 (Z-IETD-FMK (fluoromethylketone)) was purchased from Calbiochem (Darmstadt, Germany).

α4Gal-transferase Transfection—The full coding sequence of the G_b3/CD77 synthase α4Gal-T1 gene (22) was inserted into pDR2, an Epstein-Barr virus-based vector (Clontech, Palo Alto, CA) containing the hygromycin resistance gene. This construct was used to transfect Namalwa cells, which do not express G_b3/CD77. Briefly, 5 × 10⁶ Namalwa cells were transfected with 20 µg of the pDR2 or α4Gal-T1pDR2 plasmids by electroporation with a double pulse of 800 V, 25 microfarads (µF), and 100 V, 1500 µF (Easy-cell ject+, Eurogentec, France). After 48 h, cells were resuspended in RPMI 1640 supplemented with 10% fetal calf serum and 500 µg/ml hygromycin for selection. Cells were cultured for 4 weeks in this selection medium, and G_b3/CD77 antigen expression was evaluated in a FACSCalibur flow cytometer (BD Biosciences). To reduce heterogeneity in G_b3/CD77 expression on Namalwa cells transfected with the α4Gal-T1 gene, cells were relabeled with the anti-G_b3/CD77 mAb and the subset of cells with high expression levels was sorted on a FACSsort apparatus (BD Biosciences). The sorted cells were designated Nam/G_b3(+), and cells transfected with pDR2 were named NampDR2.

Induction of Apoptosis and Cell Death Measurement—We incubated 5 × 10⁵ cells with the anti-G_b3/CD77 mAb (50 µg/ml) and goat anti-mouse IgM (10 µg/ml) or with VT-1 (50 ng/ml) in 1 ml of complete RPMI 1640 medium. After 24 h at 37 °C, cells were centrifuged, resuspended in annexin buffer (10 mM HEPES/NaOH, pH 7.4, 150 mM NaCl, 5 mM KCl, 1 mM MgCl₂, 1.8 mM CaCl₂) containing 2.5 µg/ml FITC-labeled annexin V (Euromedex, France) and incubated at 4 °C for 5 min. Cells were then washed and resuspended in annexin buffer supplemented with propidium iodide (10 µg/ml) and analyzed in a FACSCalibur flow cytometer.

Measurement of Protein Synthesis—We investigated the ability of VT-1 to inhibit protein synthesis by incubating cells for 24 h in medium

containing 1 µCi/ml [³H]leucine, in the presence or absence of VT-1 (50 ng/ml) or cycloheximide (20 µg/ml) as a control for protein inhibition. Cells were harvested on glass fiber filters, and radioactivity was measured in a liquid scintillation counter (Packard, Meriden, CT).

Retrograde Transport and N-Glycosylation Analysis—Modified VT-B fragment (B-Glyc-KDEL) iodination and glycosylation analyses were carried out as previously described (23). Briefly, cells were incubated with [¹²⁵I]-B-Glyc-KDEL (20 nM) for 30 min at 4 °C and washed three times with ice-cold medium. Cells were allowed to take up iodinated VT-B for 15 h at 37 °C and were then lysed in SDS sample buffer. In some experiments, cells were treated with tunicamycin (1 µg/ml) before incubation with [¹²⁵I]-B-Glyc-KDEL. Samples were run on 10–20% polyacrylamide-SDS gradient gels, analyzed by autoradiography, and quantified with a PhosphorImager (Amersham Biosciences, Saclay, France) using ImageQuant software.

Determination of Mitochondrial Membrane Potential—We incubated 5 × 10⁵ cells with VT-1 or anti-G_b3/CD77 mAb for various periods of time. We then added carbocyanine dye, DiOC₆ (3), to a concentration of 40 nM and incubated the cells for a further 30 min at 37 °C in the dark. Cells were washed and resuspended in PBS and then analyzed in a FACSCalibur flow cytometer.

Preparation of Mitochondrial and Cytosolic Fractions—We evaluated cytochrome *c* release from the mitochondria to the cytosol by fractionating cells as previously described (24). We incubated 2 × 10⁶ cells in 100 µl of ice-cold cell lysis and mitochondria intact (CLAMI) buffer (250 mM sucrose, 70 mM KCl, 200 µg/ml digitonin in PBS) for 5 min. Cells were then collected by centrifugation (1,000 × *g* at 4 °C for 5 min) and the supernatants, containing cytosolic proteins, were stored at −80 °C. Pellets were incubated for 10 min at 4 °C in immunoprecipitation buffer (50 mM Tris-HCl, pH 7.4, 150 mM NaCl, 2 mM EDTA, 2 mM EGTA, 0.2% Triton X-100, 0.3% Nonidet P-40, complete protease inhibitor (Roche Applied Science)) and centrifuged at 10,000 × *g* for 10 min at 4 °C. The supernatants, containing mitochondrial proteins, were stored at −80 °C.

Western Blot Analysis—For PARP and caspase-8 analysis, cell pellets were solubilized in ice-cold lysis buffer (25 mM Tris HCl, pH 6.8, 1% SDS, 50 mM dithiothreitol, complete protease inhibitor (Roche Applied Science)). Sample loading buffer was added, the mixture was boiled for 5 min, and the proteins were then separated by electrophoresis on 10% polyacrylamide-SDS gels, before being transferred to PVDF membranes (Millipore) by electroblotting (Trans-blot cell, Bio-Rad). For cytochrome *c* analysis, proteins from mitochondrial and cytosolic fractions were separated by electrophoresis on a 15% polyacrylamide-SDS gel. Blots were blocked by incubation in 3% nonfat milk powder, 2% glycine in PBS and incubated for 1 h at room temperature with the primary mAb (2 µg/ml) and then with horseradish peroxidase-conjugated RAM-IgG. Antibody complexes were detected by enhanced chemiluminescence (ECL system, Amersham Biosciences).

Electron Microscopy—Cells were fixed at room temperature by adding 1.6% glutaraldehyde to the culture medium and centrifuged. Pellets were then incubated in 1.5% glutaraldehyde in 0.066 M Sorensen buffer (pH 7.4) for 1 h at 4 °C. Cells were washed for 2 h in buffer and post-fixed in 2% OsO₄ in the same buffer. They were dehydrated in a series of ethanol solutions and propylene oxide, before being embedded in Epon. Ultrathin sections, prepared with an ultramicrotome (Leica ultracut UCT, Leica Microsystems, Austria), were stained with uranyl acetate and lead citrate before observation on a Zeiss 902 microscope (Leo Electron microscopy, Rueil-Malmaison, France).

RESULTS

G_b3/CD77(+) BL Cells Display Differential Sensitivity to Apoptosis Induced by Cross-linked Anti-G_b3/CD77 mAb and VT-1—We investigated the mechanism of G_b3/CD77-mediated apoptosis by treating a series of Burkitt's lymphoma cell lines with VT-1 or an anti-G_b3/CD77 mAb (clone 1A4) cross-linked with a goat anti-mouse antibody (GAM). We selected cell lines that were spontaneously G_b3/CD77(+) (Ramos, P3HR1, BL2) or G_b3/CD77(−) (Namalwa), and we also generated G_b3/CD77(−) cells from cells that were originally positive and G_b3/CD77(+) cells from cells that were originally negative. G_b3/CD77(−) converted Ramos cells were established by treatment with PPMP, a glycolipid biosynthesis inhibitor, and are referred to as Ramos PPMP. G_b3/CD77(+) converted Namalwa cells were obtained by stable transfection with the G_b3/CD77 synthase cDNA (α4Gal-T1) (22) and are referred to as Nam/

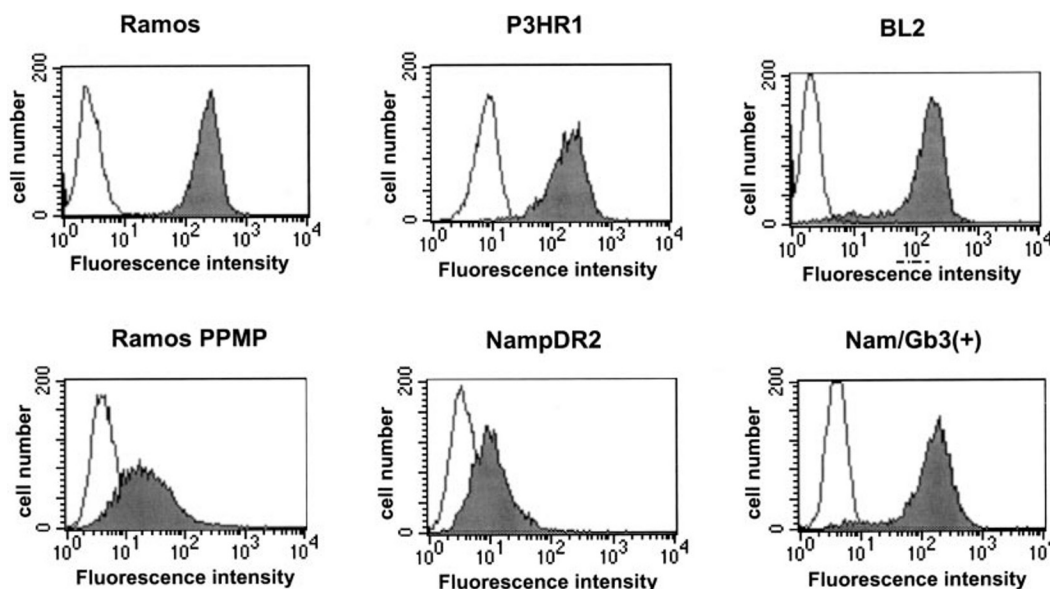


FIG. 1. Cell surface expression of G_b3/CD77 antigen in various BL cell lines. Cells were labeled with an anti-G_b3/CD77 monoclonal antibody (clone 1A4) and FITC-conjugated goat anti-mouse IgG plus IgM (shaded histograms) or with FITC-conjugated goat anti-mouse IgG plus IgM alone (open histograms). Cells were then analyzed with a FACSCalibur flow cytometer.

G_b3(+). Cell surface expression of G_b3/CD77 was evaluated by FACS analysis, using an anti-G_b3/CD77 mAb (clone 1A4). Ramos, P3HR1, BL2, and Nam/G_b3(+) cells strongly expressed G_b3/CD77 (mean fluorescence index (MFI): 228, 214, 165, and 168, respectively) (Fig. 1). The Namalwa cells transfected with the insert-less vector (NampDR2) did not express G_b3/CD77 (MFI: 14), and treatment with PPMP greatly decreased expression of this antigen (MFI: 33) (Fig. 1).

We then assessed the sensitivity of these cell lines to VT-1 and to an anti-G_b3/CD77 mAb (Table I). VT-1 and anti-G_b3/CD77 mAb had different effects: apoptosis levels were high in Ramos, BL2, and P3HR1 cells treated with anti-G_b3/CD77 mAb (74 ± 13%, 71 ± 11%, and 89 ± 5%, respectively), whereas Nam/G_b3(+) cells responded only weakly to this treatment (28 ± 4%). In contrast, VT-1 strongly induced apoptosis in Ramos, BL2, and Nam/G_b3(+) cells (98 ± 1%, 96 ± 4%, and 66 ± 7%, respectively), whereas it had almost no effect on P3HR1 cells (11 ± 3%). We investigated whether the resistance of P3HR1 to VT-1-induced apoptosis was dose-dependent by treating these cells with 500 ng/ml and 5 μg/ml VT-1. No apoptosis was observed at either concentration (data not shown). G_b3/CD77(-) NampDR2 and Ramos PPMP cells were not killed by anti-G_b3/CD77 mAb or VT-1 (Table I).

Two of the G_b3/CD77(+) BL cell lines tested (Ramos and BL2) were therefore sensitive to both anti-G_b3/CD77 mAb and VT-1; one cell line (P3HR1) was sensitive to anti-G_b3/CD77 mAb only, and one (Nam/G_b3(+)) was mostly sensitive to VT-1. Thus, the induction of apoptosis by anti-G_b3/CD77 mAb and VT-1 is strictly dependent on cell-surface G_b3/CD77 expression, but this expression is not sufficient to confer sensitivity to these apoptosis inducers.

Retrograde Transport of the VT-B Subunit Is Similar in All G_b3/CD77(+) BL Cells—To determine why P3HR1 cells do not undergo apoptosis when treated by VT-1, we investigated the pathway by which verotoxin is taken up by BL cell lines. The retrograde transport of VT to the ER has been shown to be necessary for maximal toxicity (25). We evaluated the uptake of VT into the ER, using a previously described modified VT-B subunit (B-glyc-KDEL) (23). B-glyc-KDEL carries an *N*-glycosylation site at the C terminus of the VT-B fragment, making it possible to detect its arrival in the ER by monitoring glycosy-

TABLE I
Induction of apoptosis in various BL cells by ligation of G_b3/CD77

Cells were incubated for 24 h with anti-G_b3/CD77 mAb (clone 1A4 (50 μg/ml) cross-linked with GAM (10 μg/ml) or with verotoxin 1 (VT-1, 50 ng/ml). As negative controls, cells were incubated with GAM alone or with RPMI 1640 medium. Cells were then labeled with annexin V-FITC and propidium iodide and analyzed with a FACSCalibur flow cytometer to determine the percentage of apoptotic cells.

Cell line	Apoptotic cells				
	GAM	Anti-G _b 3	Medium	VT-1	
%					
CD77(+)	Ramos	9 ± 2	74 ± 13	10 ± 3	98 ± 1
	BL2	9 ± 3	71 ± 11	9 ± 2	96 ± 4
	P3HR1	7 ± 2	89 ± 5	6 ± 1	11 ± 3
	Nam/G _b 3(+)	6 ± 2	28 ± 4	7 ± 1	66 ± 7
CD77(-)	Ramos PPMP	6 ± 1	8 ± 1	6 ± 1	13 ± 5
	NampDR2	5 ± 1	6 ± 2	6 ± 2	5 ± 1

lation by the ER-located oligosaccharyltransferase. After iodinated B-glyc-KDEL had been taken up (at 37 °C for 15 h), we lysed the cells (Ramos, P3HR1, Nam/G_b3(+), NampDR2, and HeLa (used as a positive control)) and analyzed the lysates by high resolution gradient gel (10–20%) electrophoresis and autoradiography. In addition to B-Glyc-KDEL, a band with a lower electrophoretic mobility was detected in HeLa, Ramos, P3HR1, and Nam/G_b3(+) extracts. No such band was detected in G_b3/CD77(-) NampDR2 extracts, in which B-Glyc-KDEL had not been internalized (Fig. 2). Treatment of the cells with tunicamycin, an inhibitor of *N*-glycosylation, totally abolished this band. Thus, this band corresponds to glycosylated B-Glyc-KDEL. This glycosylated product was quantified with a PhosphorImager: 21.8% of the total B-fragment was glycosylated in the control HeLa cells, 8.6% in Ramos, 10.8% in P3HR1, and 7.7% in Nam/G_b3(+). Because P3HR1 cells are resistant to VT-1-induced apoptosis, these observations suggest that the retrograde transport of the toxin to the ER is insufficient to trigger apoptosis.

VT-1 Inhibited Protein Synthesis Similarly in All G_b3/CD77(+) BL Cells—The cytotoxicity of VT-1 is generally considered to be mediated by the inhibition of protein synthesis (9). We therefore assessed protein synthesis in the various cell

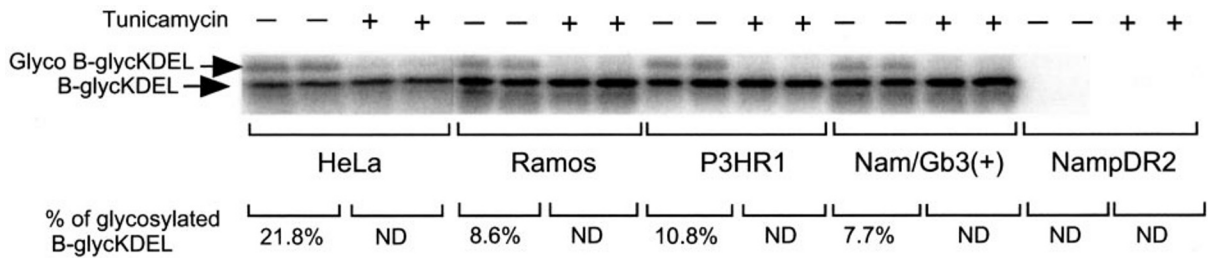


FIG. 2. **Retrograde transport of the VT-B fragment is similar in all G_b3/CD77(+) BL cells.** Cells (with or without prior tunicamycin (1 μ g/ml) treatment) were incubated with radiolabeled VT-B fragment (B-Glyc-KDEL, 20 nM) for 30 min on ice. Cells were washed, incubated at 37 $^{\circ}$ C for 15 h, and then lysed in SDS sample buffer. Lysates were subjected to electrophoresis on 10–20% polyacrylamide-SDS gradient gels, analyzed by autoradiography, and quantified with a PhosphorImager (Amersham Biosciences, Saclay, France) using ImageQuant software. ND, not detectable.

lines (Ramos, P3HR1, Nam/Gb3(+), and NampDR2) treated for 24 h with VT-1, by measuring [3 H]leucine uptake. As a control, cells were also treated with cycloheximide, a general protein synthesis inhibitor. Protein synthesis was totally inhibited in Ramos and P3HR1 cells treated with VT-1 (0.6% and 1% of the [3 H]leucine uptake of untreated cells, respectively) and almost totally inhibited in Nam/Gb3(+) cells (8.5% of the [3 H]leucine uptake of control cells). No effect was observed in the Gb3/CD77(–) NampDR2 cell line (101% of [3 H]leucine uptake) (Table II). Cycloheximide completely inhibited protein synthesis in all four BL cell lines. The results obtained with P3HR1 cells indicate that the apoptotic and protein synthesis-inhibiting effects of VT-1 can be dissociated.

VT-1 Induces Caspase Activation, whereas Cross-linked Anti-Gb3/CD77 mAb Does Not—We investigated the involvement of caspases in the apoptotic pathways induced by VT-1 and anti-Gb3/CD77 mAb. Caspase-8 is an initiator caspase involved in a variety of apoptotic pathways. We investigated its activation in our BL cells. Ramos, P3HR1, Nam/Gb3(+), and NampDR2 cells were treated with VT-1 or anti-Gb3/CD77 mAb for various periods of time (2, 4, 6, 8, and 16 h), and caspase-8 activation was assessed by Western blotting with a mAb that strongly recognized the zymogen form (54/55 kDa) and the intermediate form (41/43 kDa) and only weakly recognized the 18-kDa active subunit. Levels of the 41/43-kDa intermediate gradually increased in extracts of Ramos cells treated with VT-1 for 2–16 h, whereas levels of the zymogen decreased (Fig. 3); in P3HR1 cells, VT-1 did not induce caspase-8 cleavage, whereas in Nam/Gb3(+) cells, the 41/43-kDa intermediate form appeared after 4 h of treatment and gradually accumulated until 16 h. No caspase-8 cleavage was observed in the three cell lines treated with anti-Gb3/CD77 mAb (see Fig. 3) or in Gb3/CD77(–) NampDR2 cells treated with VT-1 or anti-Gb3/CD77 mAb (data not shown).

Caspase-8 cleaves and activates caspase-3. Thus, we investigated the cleavage of poly(ADP-ribose) polymerase (PARP), a DNA repair enzyme directly targeted by caspase-3. In Ramos cells, the 85-kDa PARP proteolytic product was detected on Western blots after 2 h of treatment with VT-1 and increased in amount until 8 h of treatment, when native PARP protein was no longer detected (Fig. 4). In P3HR1 cells, a small amount of the 85-kDa cleavage product was detected only after 16 h of treatment with VT-1. In Nam/Gb3(+) cells, the 85-kDa band was first detected after 4 h of treatment and increased in intensity until 16 h. However, unlike in Ramos cells, the native form was never totally cleaved in these cells. Treatment of these three cell lines with anti-Gb3/CD77 mAb did not induce cleavage of the PARP protein. Treatment of NampDR2 cells with VT-1 or anti-Gb3/CD77 mAb did not result in PARP cleavage (data not shown). Thus, caspases are involved in the apoptotic pathway induced by VT-1, whereas the mechanism of anti-Gb3/CD77 mAb-induced apoptosis seems to be caspase-independent.

VT-1 and Cross-linked Anti-Gb3/CD77 mAb Induce a Loss of Mitochondrial Membrane Potential in Different Ways—Mitochondria are a key element in many apoptotic pathways (reviewed in Ref. 26). We therefore measured mitochondrial membrane potential ($\Delta\psi_m$) before and after treatment of the cells with VT-1 or anti-Gb3/CD77 mAb. We measured $\Delta\psi_m$ by cytofluorimetry, using the carbocyanine dye DiOC₆(3). In Ramos cells, VT-1 induced a loss of $\Delta\psi_m$ after 4 h of treatment, which gradually increased until 16 h, when mitochondrial membrane depolarization was observed in all cells (Fig. 5A). In Nam/Gb3(+) cells, the loss of $\Delta\psi_m$ was delayed, and only 18% of cells were DiOC₆(3)^{low} after 8 h of treatment. However, $\Delta\psi_m$ loss then rapidly increased and 66% of cells were DiOC₆(3)^{low} after 24 h of treatment. No $\Delta\psi_m$ loss was observed in P3HR1 and NampDR2 cells. We investigated whether caspase-8 activation occurred upstream or downstream from mitochondrial perturbation by studying the effects of a caspase-8-specific inhibitor (Z-IETD-fmk) on $\Delta\psi_m$ loss. Preincubation of the cells with this tetrapeptide inhibited the loss of $\Delta\psi_m$ induced by VT-1 (after 24 h, 69% of pre-treated Ramos cells were DiOC₆(3)^{low} versus 100% of cells that had not been pre-treated, and 48% of pre-treated Nam/Gb3(+) cells were DiOC₆(3)^{low} versus 66% of non-pre-treated cells) (Fig. 5A). Thus, mitochondrial depolarization appears to depend, at least partly, on caspase-8 activation.

We also treated the BL cell lines for the same length of time with anti-Gb3/CD77 mAb. Anti-Gb3/CD77 mAb induced a moderate, sustained loss of $\Delta\psi_m$ in P3HR1 cells (~30% of the cells were DiOC₆(3)^{low} following 4–24 h of treatment) but had no effect on $\Delta\psi_m$ in Ramos cells (although these cells are as sensitive as P3HR1 to anti-Gb3/CD77 mAb) or on $\Delta\psi_m$ in Nam/Gb3(+) and NampDR2 cells (Fig. 5B).

VT-1 and Cross-linked Anti-Gb3/CD77 mAb Induce Cytochrome c Release from Mitochondria in Different Ways—During apoptosis, $\Delta\psi_m$ disruption is generally accompanied by the release of cytochrome *c* from the mitochondria to the cytoplasm, where it forms complexes with Apaf-1, dATP, and caspase-9. This activates caspase-9, which in turn activates caspase-3. We investigated cytochrome *c* release following treatment with VT-1 and anti-Gb3/CD77 mAb by treating BL cell lines for various lengths of time (2, 4, 6, 8, 16, and 24 h) and preparing subcellular fractions as previously described (24). Western blot analysis of the cytosolic and mitochondrial fractions was carried out using an anti-cytochrome *c* mAb (Fig. 6). Cytochrome *c* levels in the mitochondrial fractions of Ramos cells treated with VT-1 decreased slightly after 4 h of treatment, were only just detectable after 6 h, and were completely undetectable after 8, 16, and 24 h. Conversely, cytochrome *c* was first detected in the cytosolic fractions of these cells after 2 h of treatment, and its levels gradually increased until 24 h. No changes in cytochrome *c* levels were observed in the mitochondrial or cytosolic fractions of cells treated with anti-Gb3/CD77 mAb, other than slight changes after 24 h of treatment. In

TABLE II
Analysis of protein synthesis after treatment with VT-1

Cells were incubated for 24 h with or without VT-1 (50 ng/ml) in medium containing 1 μ Ci/ml [³H]leucine. As a control for protein inhibition, cells were incubated with cycloheximide (20 μ g/ml). Cells were then harvested on glass fiber filters, and radioactivity was measured in a liquid scintillation counter.

Cell line	³ H]Leucine uptake (% of control)		
	Control	VT-1	Cycloheximide
Ramos	103,623 \pm 8,161	589 \pm 105 (0.6%)	479 \pm 63 (0.5%)
P3HR1	96,204 \pm 9,840	989 \pm 242 (1%)	1,979 \pm 275 (2%)
Nam/Gb3(+)	82,794 \pm 15,505	7,039 \pm 785 (8.5%)	1,568 \pm 206 (1.9%)
NampDR2	89,849 \pm 11,863	90,506 \pm 9,796 (101%)	1,357 \pm 299 (1.5%)

FIG. 3. VT-1, but not anti-Gb3/CD77 mAb, induces caspase-8 activation. Cells were treated with VT-1 or an anti-Gb3/CD77 mAb (clone 1A4 cross-linked with GAM) for various periods of time. Cell pellets were then solubilized, and equal amounts of proteins were subjected to electrophoresis on a 10% polyacrylamide-SDS gel. Proteins were then transferred to PVDF membranes, which were probed with an anti-caspase-8 mAb and a horseradish peroxidase-conjugated rabbit anti-mouse Ig antibody. Antibody complexes were detected by enhanced chemiluminescence.

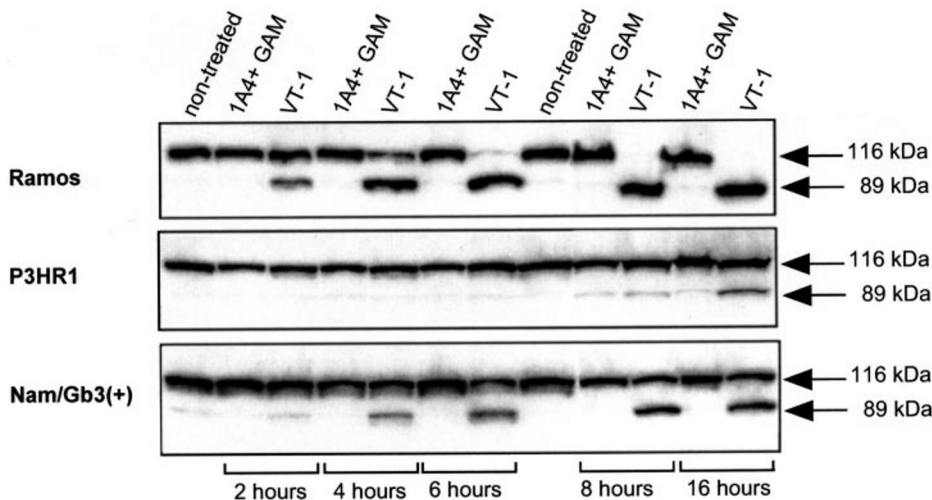
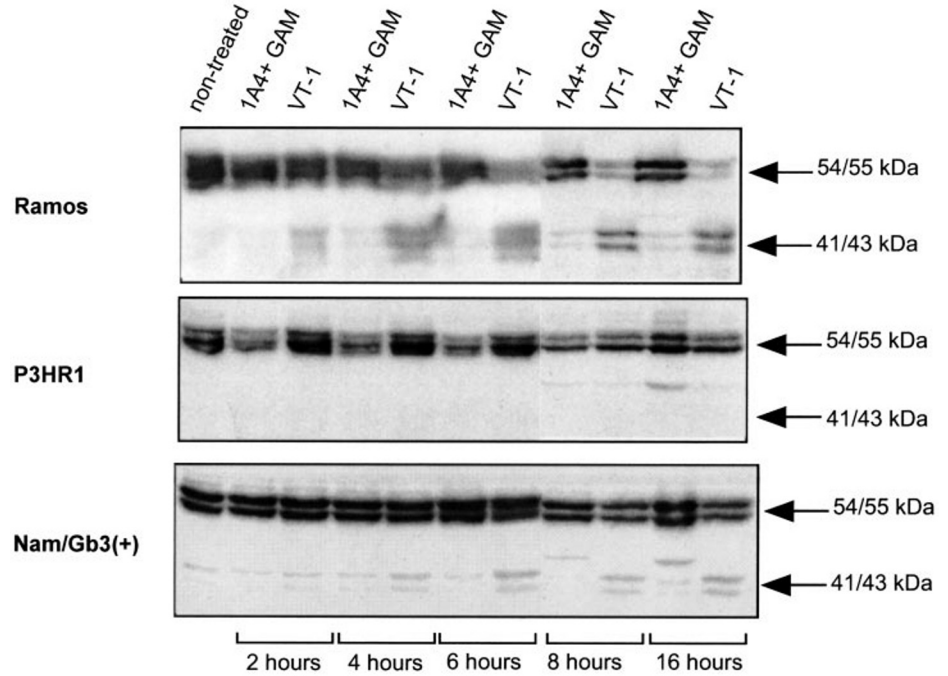


FIG. 4. VT-1, but not anti-Gb3/CD77 mAb, induces cleavage of the PARP protein. Cells were treated with either VT-1 or an anti-Gb3/CD77 mAb (clone 1A4 cross-linked with GAM) for various periods of time. Cell pellets were then solubilized and equal amounts of protein were subjected to electrophoresis on a 10% polyacrylamide-SDS gel. Proteins were then transferred to PVDF membranes, which were probed with an anti-PARP (a target of activated caspase-3) mAb and a horseradish peroxidase-conjugated rabbit anti-mouse Ig antibody. Antibody complexes were detected by enhanced chemiluminescence.

P3HR1 cells treated with VT-1, no significant changes in cytochrome *c* levels were observed in the mitochondrial or cytosolic fractions. By contrast, cytochrome *c* became clearly detectable in the cytosolic fraction of these cells after 4 h of treatment with anti-Gb3/CD77 mAb. However, this release appeared to be moderate as no clear decrease in cytochrome *c* level was observed in the mitochondrial fraction. The cytochrome *c* levels in the mitochondrial fraction of NamG_b3(+) cells treated with VT-1 clearly decreased 4 h after treatment and was accompanied by an increase in cytochrome *c* levels in the cytosolic

fraction. Treatment of these cells with anti-Gb3/CD77 mAb did not change the cytochrome *c* levels. Thus, VT-1 induces the concomitant release of cytochrome *c* and loss of $\Delta\psi_m$. Our results also show that in P3HR1, but not in Ramos cells, anti-Gb3/CD77 mAb induces a moderate depolarization of mitochondria, together with a release of cytochrome *c* without caspase activation.

Cells Treated with VT-1 and Cross-linked Anti-Gb3/CD77 mAb Display Different Morphological Changes—We used electron microscopy to investigate Ramos cells, which are sensitive

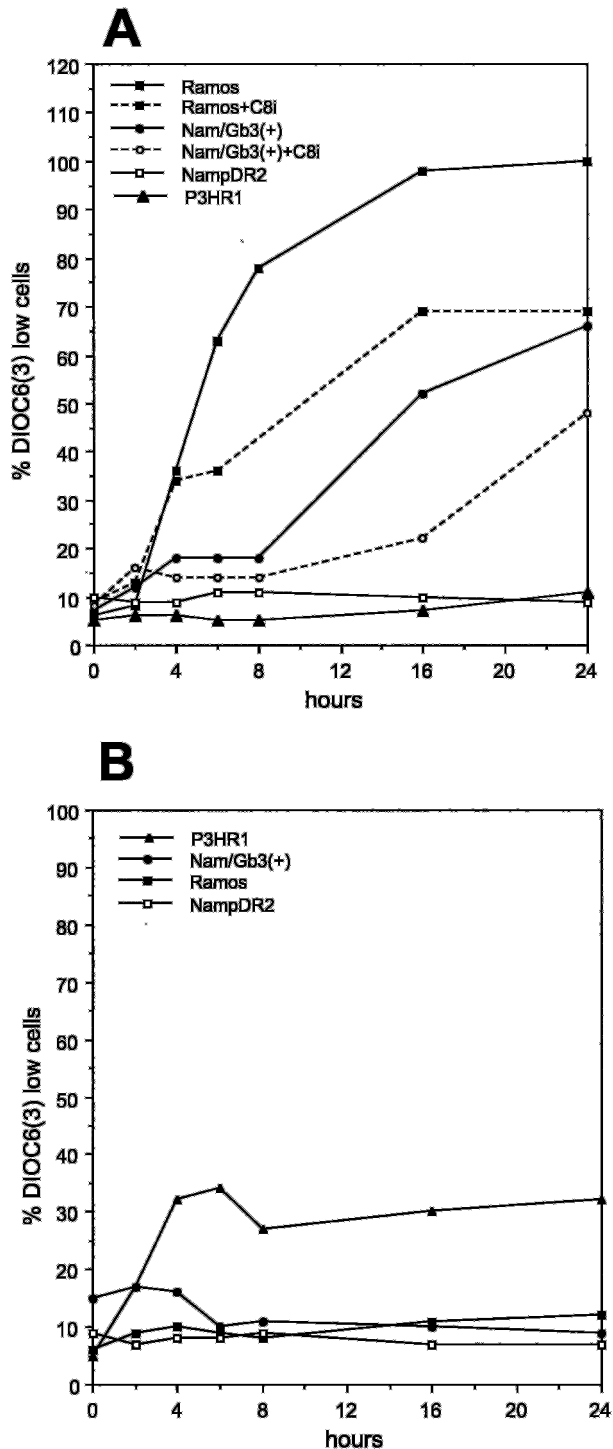


FIG. 5. Loss of mitochondrial membrane potential ($\Delta\psi_m$) following treatment with VT-1 or anti-Gb3/CD77 mAb. A, cells were either directly treated with VT-1 or incubated with a caspase-8-specific inhibitor (C8i) before being treated with VT-1. B, cells were treated with an anti-Gb3/CD77 mAb (clone 1A4 cross-linked with GAM). After various periods of time, cells were stained with DiOC₆(3) and analyzed on a FACSCalibur flow cytometer. DiOC₆(3) stain mitochondria in a potential-dependent fashion. Cells with a low $\Delta\psi_m$ are therefore poorly fluorescent and are called "DiOC₆(3) low."

to both VT-1- and anti-Gb3/CD77 mAb-induced apoptosis. The morphological features of cells treated with VT-1 (Fig. 7, B and E) and anti-Gb3/CD77 mAb (Fig. 7, C and F) were very different. Cells treated with VT-1 were smaller than control cells (Fig. 7, A and D). They also presented classic heavy condensation of chromatin into globular or crescent-shaped figures, and

large cytosolic vacuoles. Cells treated with anti-Gb3/CD77 mAb were also small but, unlike VT-1-treated cells, they had lost their rounded shapes, showed less compact chromatin condensation (with more complex, lumpier shapes), and the cytosolic vacuoles were smaller and more numerous. These features are reminiscent of those described by several authors for caspase-independent apoptosis (for review see Ref. 27).

The Antioxidants NAC and GSH Protect BL Cells Strongly from Anti-Gb3/CD77 mAb-induced Apoptosis but Barely from VT-1-induced Apoptosis—The intracellular regulation of redox processes seems to be involved in cell death induced by various stimuli. Several studies have demonstrated that reactive oxygen species (ROS) regulate many important cellular events, including apoptosis (reviewed in Refs. 28 and 29) and that various antioxidants block apoptosis (30). We therefore investigated the effects of two antioxidant agents, NAC and GSH-EE (a cell-permeable form of reduced glutathione), on the percentage of apoptotic cells induced by anti-Gb3/CD77 mAb and VT-1. Because NAC and GSH-EE were toxic to Ramos cells, we used BL2 cells, which are also sensitive to both anti-Gb3/CD77 mAb and VT-1 (see Table I). Pre-treatment of the cells for 2 h with 20 mM NAC partially or almost completely protected cells (BL2, Nam/Gb3(+), and P3HR1 cells, respectively) from the apoptosis induced by anti-Gb3/CD77 mAb, but had no effect (BL2 cells) or only a slight effect (Nam/Gb3(+) cells) on VT-1-induced apoptosis (Fig. 8). Preincubation of P3HR1 and Nam/Gb3(+) cells with 15 mM GSH EE gave similar results, with slightly stronger protection for VT-1-treated Nam/Gb3(+) cells. Thus, ROS are important elements of the apoptotic pathway induced by anti-Gb3/CD77 mAb, whereas they play little or no role in the pathway induced by VT-1.

DISCUSSION

Disruption of the gene encoding glucosylceramide (the source of most GSL) synthase leads to embryonic lethality (31), showing that GSL are essential for many cellular processes (reviewed in Refs. 32 and 33). However, many studies (including some investigating the inactivation of other glycosyltransferases (34)) have also shown that the mediation of signals by GSL is highly complex. At the cell surface, signal transduction by GSL depends on the structure and association of these molecules with transducer molecules and on their intracellular routing after uptake. Gb3/CD77, a neutral GSL, has been extensively studied and shown to transduce apoptotic signals following the binding of various ligands: the Stx holotoxin, the recombinant binding subunit of Stx and anti-Gb3/CD77 mAb (6, 13, 15, 35, 36). We investigated the mechanisms of Gb3/CD77-mediated apoptosis by comparing the signaling pathways induced by one member of the Stx family (VT-1) and by an anti-Gb3/CD77 mAb in various BL cell lines.

We found that both pathways were strictly receptor-dependent, but that the presence of the receptor is not sufficient to trigger apoptosis. Our results also demonstrate that the VT-1- and anti-Gb3/CD77-induced pathways are completely independent (results are summarized in Tables III and IV). These data are the first to show that a cell can be resistant to one CD77 ligand and sensitive to another and that a glycosphingolipid can mediate two different cell death pathways. Our data confirm previous reports that caspases are involved in VT-1-induced apoptosis (18, 19, 37). We also showed that VT-1 triggered mitochondrial changes that, in part, rely on caspase-8 activation. The mechanism of this activation is currently unclear.

We found that, in apoptosis-resistant P3HR1 cells, VT-1 underwent retrograde transport to the ER as efficiently as in sensitive BL cells. Thus, either delivery of the toxin to the ER is not a key step in apoptosis induction or induction occurs after

FIG. 6. Release of cytochrome *c* from mitochondria after treatment with VT-1 or anti-G_b3/CD77 mAb. Cells were treated with either VT-1 or an anti-G_b3/CD77 mAb (clone 1A4 cross-linked with GAM) for various periods of time and then fractionated into mitochondrial and cytosolic fractions as described under "Experimental Procedures." Equal amounts of each fraction (20 μ g of mitochondrial protein and 40 μ g of cytosolic protein) were subjected to electrophoresis on a 15% polyacrylamide-SDS gel. Proteins were then transferred to PVDF membranes, which were probed with an anti-cytochrome *c* mAb and a horseradish peroxidase-conjugated rabbit anti-mouse Ig antibody. Antibody complexes were detected by enhanced chemiluminescence.

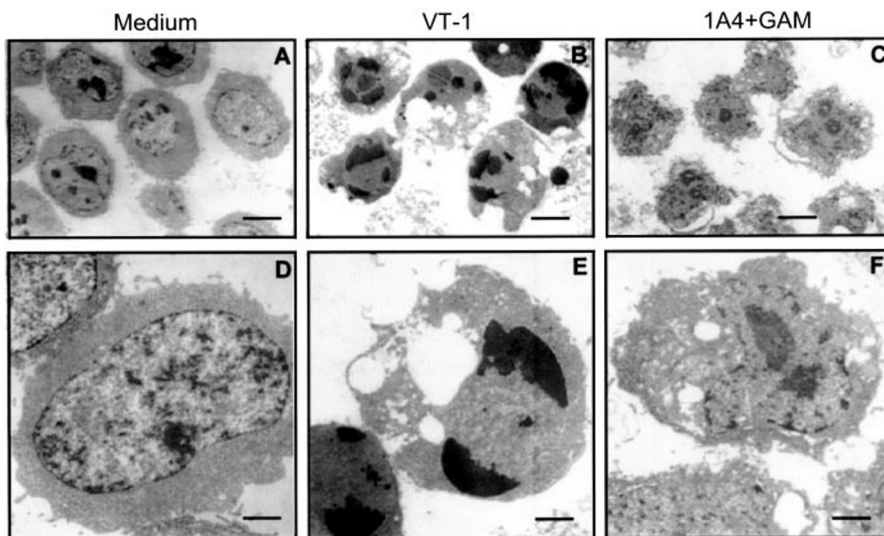
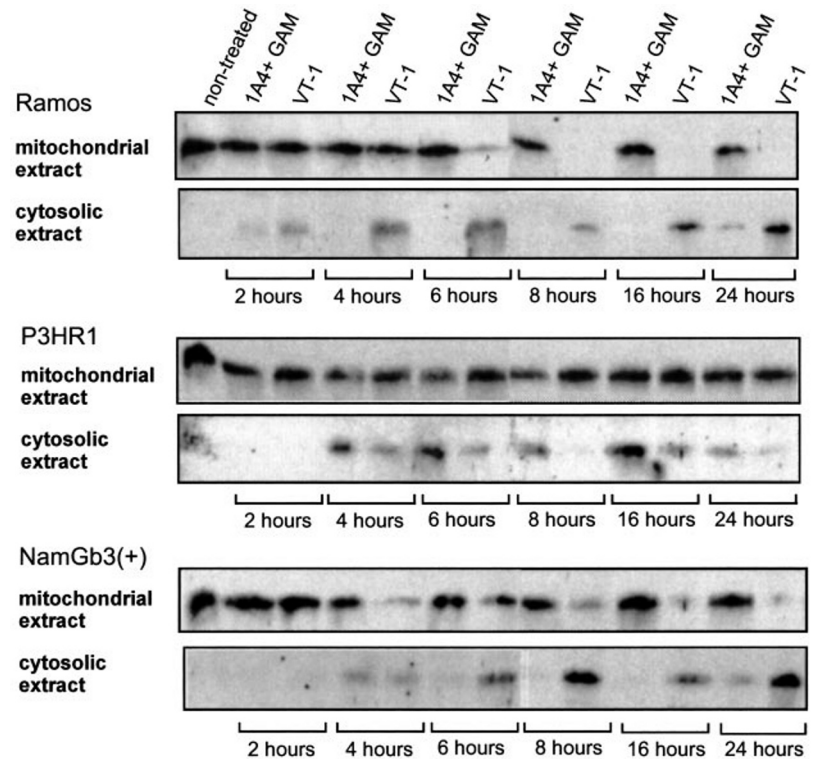


FIG. 7. Cells treated with VT-1 and anti-G_b3/CD77 mAb displayed different morphological changes. Ramos cells were cultured for 24 h in RPMI 1640 medium alone (A and D), 16 h in the presence of VT-1 (B and E), or 24 h in the presence of an anti-G_b3/CD77 mAb (clone 1A4 cross-linked with GAM) (C and F), and then fixed in isotonic 1.6% glutaraldehyde solution. Electron micrographs of thin, plastic-embedded sections were taken on a Philips EM 400 electron microscope. Bars, 2.7 μ m (A–C) and 1 μ m (D–F).

VT-1 reaches the ER. The second of these two possibilities is the most likely as treatment of the cells with brefeldin A (a fungal metabolite that provokes disassembly of the Golgi apparatus) inhibits VT-induced apoptosis (13, 37). Our data therefore imply that, in resistant cells, apoptosis is inhibited after delivery of the toxin to the ER.

The efficient inhibition of protein synthesis by VT-1 in P3HR1 cells, in the absence of apoptosis, provides new insight into the relationship between these two processes. Although it remains possible that protein synthesis inhibition triggers apoptosis, our data strongly suggest that these two processes are independent. Furthermore, the rapid activation of caspases and mitochondria in sensitive cells are also consistent with this. Various studies have already addressed this issue and have generated conflicting conclusions: apoptosis induced by the B subunit alone has led some authors to conclude that protein synthesis inhibition and apoptosis are independent (5, 12, 13), whereas another study, in which the VT-1 B chain did

not induce apoptosis (10), led to the opposite conclusion. Other studies with VT-1 and cycloheximide also came to conflicting conclusions (11, 38, 39). We are currently comparing the abilities of various protein synthesis inhibitors and VT-1 to induce apoptosis in a panel of G_b3/CD77(+) BL cells.

The prior incubation of BL cells with antioxidant compounds strongly protected against anti-G_b3/CD77-induced apoptosis. Oxidative stress has been shown to mediate apoptosis in several independent experiments (reviewed in Ref. 29). In these experiments, oxidants induced apoptosis (40), ROS were generated during apoptosis (41), or antioxidants blocked apoptosis (29, 42). We show here that two antioxidants, NAC and GSH, strongly protected the cells against apoptosis induced by anti-G_b3/CD77 mAb. We also recently observed that preincubation with L-buthioninesulfoximine (a specific inhibitor of GSH synthesis) sensitizes Ramos and P3HR1 cells to low doses of anti-G_b3/CD77 mAb (5 and 15 μ g/ml) (data not shown), thereby confirming that GSH is an important regulator of anti-G_b3/

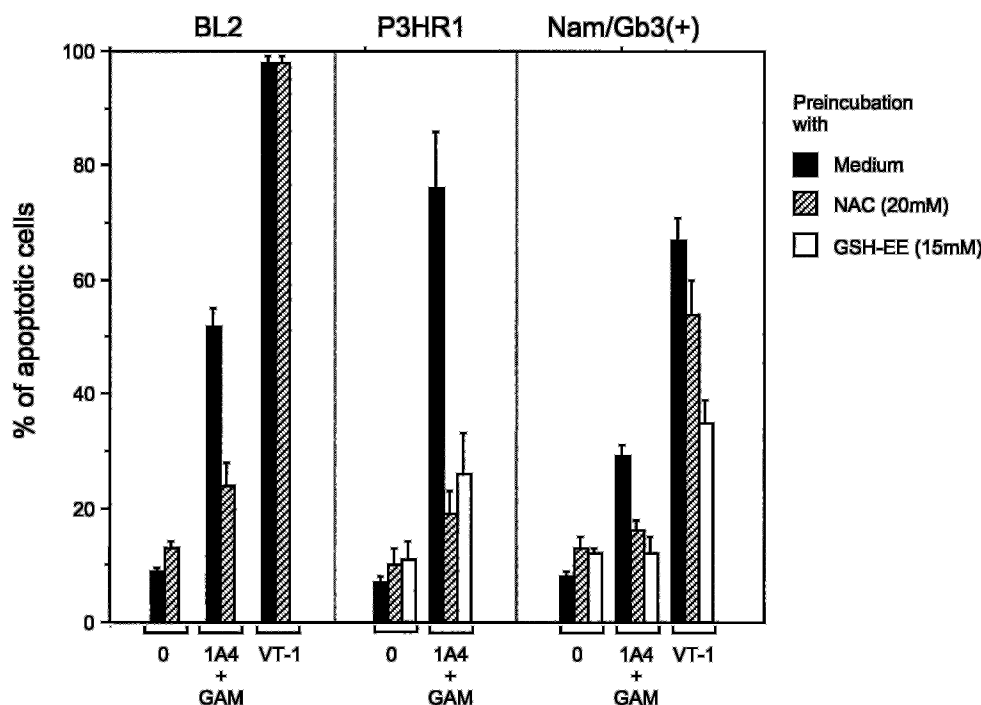


FIG. 8. Antioxidants protect BL cells strongly from anti-G_b3/CD77 mAb-induced apoptosis but only slightly from VT-1-induced apoptosis. Cells were incubated for 2 h with medium, *N*-acetyl-L-cysteine (NAC) or glutathione ethyl ester (GSH-EE, a cell-permeable form of reduced glutathione) and were then treated with VT-1 or an anti-G_b3/CD77 mAb (clone 1A4 cross-linked with GAM). After 24 h, cells were labeled with annexin V-FITC and propidium iodide and analyzed with a FACSCalibur flow cytometer to determine the percentage of apoptotic cells.

TABLE III
General characteristics of the BL cell lines

Cell line	G _b 3/CD77 expression	Apoptosis sensitivity		Transport of VT-B fragment	Protein synthesis inhibition by VT-1
		Anti-G _b 3	VT-1		
Ramos	+++	+++	+++	++ ^a	+++
P3HR1	+++	+++	—	++	+++
Nam/Gb3(+)	++	+	++	++	+++
NampDR2	—	—	—	—	—
Ramos PMP	—	—	—	ND ^b	ND

^a ++ indicates that the transport of the VT-B fragment to ER was slightly less efficient than in control HeLa cells.

^b ND, not determined.

TABLE IV
Characteristics of the apoptotic pathways induced by VT1 and anti-G_b3/CD77 mAb in BL cells

	VT-1	Anti-G _b 3/CD77 mAb
Caspase activation	++	—
Loss of $\Delta\psi_m$	++	+/- ^a
Cytochrome <i>c</i> release	++	+/- ^a
Chromatin condensation	++	+
Antioxidant protection	+/- ^a	++

^a Low or negative depending on the cell line.

CD77-induced apoptosis and substantiating the role of redox reactions in this process.

ROS production and ceramide generation were recently shown to be closely linked: ceramide generation was shown to be a redox-sensitive process (through regulation of the neutral sphingomyelinase) and ROS, produced by mitochondria, were shown to be early mediators of ceramide-induced cell death (43, 44). It was also shown that the addition of ceramide to isolated mitochondria induces cytochrome *c* release and the loss of $\Delta\psi_m$ (45). Because ceramide accumulates in BL cells exposed to an anti-G_b3/CD77 mAb (6), we are now conducting experiments to confirm the role of oxidative stress in anti-G_b3/CD77 mAb-induced apoptosis and to determine the contribution of ceramide to this signaling pathway. However, as some glycosphingolipids (GD3 and LacCer) also induce ROS formation, a decrease

in $\Delta\psi_m$, and the release of cytochrome *c* from mitochondria (46), we are currently testing the effect of G_b3/CD77 on isolated mitochondria.

In conclusion, we demonstrate here that two different apoptotic pathways are triggered depending of the nature of the ligand binding to the G_b3/CD77 glycosphingolipid receptor: a caspase- and mitochondria-dependent pathway or a ROS-dependent pathway.

Acknowledgments—We thank Naoufal Zamzami for helpful advice and Marc Lipinski for critical reading of the manuscript and suggestions.

REFERENCES

- Marcus, D. M., Kundu, S. K., and Suzuki, A. (1981) *Sem. Hematol.* **18**, 63–71
- Mangeney, M., Richard, Y., Coulaud, D., Tursz, T., and Wiels, J. (1991) *Eur. J. Immunol.* **21**, 1131–1140
- Hardie, D. L., Johnson, G. D., Khan, M., and MacLennan, I. C. (1993) *Eur. J. Immunol.* **23**, 997–1004
- Paton, J. C., and Paton, A. W. (1998) *Clin. Microbiol. Rev.* **11**, 450–479
- Mangeney, M., Lingwood, C. A., Taga, S., Caillou, B., Tursz, T., and Wiels, J. (1993) *Cancer Res.* **53**, 5314–5319
- Taga, S., Carlier, K., Mishal, Z., Capoulade, C., Mangeney, M., Lécluse, Y., Coulaud, D., Tétaud, C., Pritchard, L. L., Tursz, T., and Wiels, J. (1997) *Blood* **90**, 2757–2767
- Lingwood, C. A. (1996) *Trends Microbiol.* **4**, 147–153
- O'Brien, A. D., Tesh, V. L., Donohue-Rolfe, A., Jackson, M. P., Olsnes, S., Sandvig, K., Lindberg, A. A., and Keusch, G. T. (1992) *Curr. Top. Microbiol. Immunol.* **180**, 65–94

9. Endo, Y., Tsurugi, K., Yutsudo, T., Takeda, Y., Ogasawara, T., and Igarashi, K. (1988) *Eur J Biochem.* **171**, 45–50
10. Williams, J. M., Lea, N., Lord, J. M., Roberts, L. M., Milford, D. V., and Taylor, C. M. (1997) *Toxicol. Lett.* **91**, 121–127
11. Taguchi, T., Uchida, H., Kiyokawa, N., Mori, T., Sato, N., Horie, H., Takeda, T., and Fujimoto, J. (1998) *Kidney Int.* **53**, 1681–1688
12. Arab, S., Murakami, M., Dirks, P., Boyd, B., Hubbard, S. L., Lingwood, C. A., and Rutka, J. T. (1998) *J. Neurooncol.* **40**, 137–150
13. Marcato, P., Mulvey, G., and Armstrong, G. D. (2002) *Infect. Immun.* **70**, 1279–1286
14. Johannes, L., and Goud, B. (2000) *Traffic* **1**, 119–123
15. Sandvig, K. (2001) *Toxicol.* **39**, 1629–1635
16. Arab, S., and Lingwood, C. A. (1998) *J. Cell. Physiol.* **177**, 646–660
17. Falguères, T., Mallard, F., Baron, C., Hanau, D., Lingwood, C. A., Goud, B., Salamero, J., and Johannes, L. (2001) *Mol. Biol. Cell* **12**, 2453–2468
18. Ching, J. C., Jones, N. L., Ceponis, P. J., Karmali, M. A., and Sherman, P. M. (2002) *Infect. Immun.* **70**, 4669–4677
19. Kiyokawa, N., Mori, T., Taguchi, T., Saito, M., Mimori, K., Suzuki, T., Sekino, T., Sato, N., Nakajima, H., Katagiri, Y. U., Takeda, T., and Fujimoto, J. (2001) *J. Cell. Biochem.* **81**, 128–142
20. Abe, A., Inokuchi, J., Jimbo, M., Shimeno, H., Nagamatsu, A., Shayman, J. A., Shukla, G. S., and Radin, N. S. (1992) *J. Biochem. (Tokyo)* **111**, 191–196
21. Kojima, H., Tsuchiya, S., Sekiguchi, K., Gelinas, R., and Hakomori, S. (1987) *Biochem. Biophys. Res. Commun.* **143**, 716–722
22. Steffensen, R., Carlier, K., Wiels, J., Levery, S. B., Stroud, M., Cedergren, B., Sojka, B. N., Bennett, E. P., Jersild, C., and Clausen, H. (2000) *J. Biol. Chem.* **275**, 16723–16729
23. Johannes, L., Tenza, D., Antony, C., and Goud, B. (1997) *J. Biol. Chem.* **272**, 19554–19561
24. Waterhouse, N. J., Goldstein, J. C., von Ahsen, O., Schuler, M., Newmeyer, D. D., and Green, D. R. (2001) *J. Cell Biol.* **153**, 319–328
25. Sandvig, K., and van Deurs, B. (2000) *EMBO J.* **19**, 5943–5950
26. Kroemer, G., and Reed, J. C. (2000) *Nat. Med.* **6**, 513–519
27. Leist, M., and Jaattela, M. (2001) *Nat. Rev. Mol. Cell. Biol.* **2**, 589–598
28. Suzuki, Y. J., Forman, H. J., and Sevanian, A. (1997) *Free Radic. Biol. Med.* **22**, 269–285
29. Chandra, J., Samali, A., and Orrenius, S. (2000) *Free Radic. Biol. Med.* **29**, 323–333
30. Deas, O., Dumont, C., Mollereau, B., Metivier, D., Pasquier, C., Bernard-Pomier, G., Hirsch, F., Charpentier, B., and Senik, A. (1997) *Int. Immunol.* **9**, 117–125
31. Yamashita, T., Wada, R., Sasaki, T., Deng, C., Bierfreund, U., Sandhoff, K., and Proia, R. L. (1999) *Proc. Natl. Acad. Sci. U. S. A.* **96**, 9142–9147
32. Hakomori, S., and Igarashi, Y. (1995) *J. Biochem. (Tokyo)* **118**, 1091–1103
33. Varki, A. (1993) *Glycobiology* **3**, 97–130
34. Muramatsu, T. (2000) *J. Biochem. (Tokyo)* **127**, 171–176
35. Brigotti, M., Alfieri, R., Sestili, P., Bonelli, M., Petronini, P. G., Guidarelli, A., Barbieri, L., Stirpe, F. F. A. U., and Sperti, S. (2002) *FASEB J.* **16**, 365–372
36. Nakagawa, I., Nakata, M., Kawabata, S., and Hamada, S. (1999) *Mol. Microbiol.* **33**, 1190–1199
37. Kojio, S., Zhang, H., Ohmura, M., Gondaira, F., Kobayashi, N., and Yamamoto, T. (2000) *FEMS Immunol. Med. Microbiol.* **29**, 275–281
38. Sandvig, K., and van Deurs, B. (1992) *Exp. Cell Res.* **200**, 253–262
39. Pijpers, A. H., van Setten, P. A., van den Heuvel, L. P., Assmann, K. J., Dijkman, H. B., Pennings, A. H., Monnens, L. A., and van Hinsbergh, V. W. (2001) *J. Am. Soc. Nephrol.* **12**, 767–778
40. Hampton, M. B., and Orrenius, S. (1997) *FEBS Lett.* **414**, 552–556
41. Gorman, A., McGowan, A., and Cotter, T. G. (1997) *FEBS Lett.* **404**, 27–33
42. Andrieu-Abadie, N., Gouazé, V., Salvayre, R., and Levade, T. (2001) *Free Radic. Biol. Med.* **31**, 717–728
43. Liu, B., Andrieu-Abadie, N., Levade, T., Zhang, P., Obeid, L. M., and Hannun, Y. A. (1998) *J. Biol. Chem.* **273**, 11313–11320
44. Quillet-Mary, A., Jaffrézou, J. P., Mansat, V., Bordier, C., Naval, J., and Laurent, G. (1997) *J. Biol. Chem.* **272**, 21388–21395
45. Ghafourifar, P., Klein, S. D., Schucht, O., Schenk, U., Pruschy, M., Rocha, S., and Richter, C. (1999) *J. Biol. Chem.* **274**, 6080–6084
46. Garcia-Ruiz, C., Colell, A., Paris, R., and Fernandez-Checa, J. C. (2000) *FASEB J.* **14**, 847–858